ELECTROCHEMICAL BEHAVIOUR OF MIXED LB FILMS OF UBIQUINONE-DPPC

Javier Hoyo[1], Ester Guaus[1], Juan Torrent-Burgués[1,2,4] and Fausto Sanz[2,3,4]

[1]*Universitat Politècnica de Catalunya, Dpto. Ingeniería Química, 08222 Terrassa (Barcelona,) Spain*

[2]*Instituto de Bioingeniería de Cataluña (IBEC), 08028 Barcelona, Spain*

[3]*Universitat de Barcelona, Dpto. Química-Física, 08028 Barcelona, Spain*

[4] *CIBER-BBN, Campus Rio Ebro-Edificio I+D, 50018 Zaragoza, Spain*

Email: ester.guaus@upc.edu

Abstract

The structure and the electrochemical behaviour of Langmuir and Langmuir-Blodgett (LB) films of the biological ubiquinone-10 (UQ) and a mixture of dipalmytoilphosphatidylcholine (DPPC) and UQ at the molar ratios DPPC:UQ 5:1 and 10:1 have been investigated. The surface pressure-area isotherms of the Langmuir films and the AFM images of the LB films show the formation of a monolayer in the DPPC:UQ mixture till a certain surface pressure is attained, and then at higher surface pressures the UQ is progressively expelled. The cyclic voltammograms of DPPC:UQ LB films formed on indium tin oxide, ITO, at different surface pressures show one reduction and one oxidation peak at low surface pressures, but two or even more reduction and oxidations peaks at medium and high surface pressures. The electrochemical behaviour is correlated with the film structure.

Keywords

Ubiquinone, lipid monolayer, Langmuir-Blodgett, cyclic voltammetry, electron transfer, modified ITO electrode.

1. Introduction

The understanding of electron transport processes in biological membranes is one of the current challenges to mimic natural processes. Focusing the attention in bioenergetics processes, ubiquinone-10 (UQ) and plastoquinone-9 are known to be an important kind of natural quinones involved in the respiratory and photosynthetic pathways of the mitochondrial and thylakoid membranes, respectively [1-3]. In particular, the UQ molecule contains a quinone redox centre (head) and a long isoprenoid chain (tail) of ten isoprenoid units (Scheme 1). This tail confers a high hydrophobic character to the molecule.

Scheme 1. Ubiquinone-10

In order to study the electrochemical behaviour of the ubiquinone-10 (UQ)/ubiquinol-10 (UQH$_2$) redox couple in an environment that mimic the biological membranes, some important aspects must be understood like reproducing the structure of the lipid bilayer, inserting the UQ molecules in the lipid membrane and controlling the redox state of the UQ/UQH$_2$ couple. One of the first attempts to study the electrochemistry of UQ in this kind of environments used lipid monolayer and bilayer systems supported on Hg as biological membrane models [4]. Using such systems Guidelli et al. [5, 6] and Gordillo et al. [7, 8] studied the electrochemistry of UQ on a phospholipid monolayer by chronocoulometry and cyclic voltammetry. On solid electrodes, different methods have been applied to modify the surface of the electrode with a thin layer simulating the structure of the lipid layer [9], where the quinone molecules can be embedded. The Langmuir-Blodgett (LB) and the vesicle fusion methods have been the most often applied to generate supported lipid bilayers [10-18]. Bilayers so obtained have been used to study the electron transport properties of UQ [19, 20], duroquinone [21] and naphtoquinone derivatives [22] by voltammetry. Other techniques like cast coating [23, 24], black lipid membrane (BLM) [25], and other thin layer approaches [26-29] have also been used to study the voltammetric behaviour of UQ and other quinone derivatives.

2

As a result of all these studies, the thermodynamic properties of the UQ/UQH$_2$ redox couple in different model systems have been reported, but one important factor as the location of the ubiquinone molecules in the membrane during the redox process is still unclear. As the electron and proton transfers involving the quinone moiety depend on the availability of water molecules for the redox centre whereas a lipid environment should be available for the tail, the Langmuir technique offers a unique way to control these factors through the lipid film formation and compression. Moreover the orientation of the phospholipid molecules will depend on the hydrophobic/hydrophilic character of the surface. Therefore when the LB film is transferred on an indium tin oxide (ITO) electrode, which is hydrophilic, the obtained lipid film structure, with the polar phosphatidyl groups towards the electrode surface [10], is very different to that obtained on a mercury electrode [9], which is hydrophobic having the hydrocarbon chains towards the electrode surface.

The surface-active properties of ubiquinone monolayers, and mixed ubiquinone-phospholipid monolayers were investigated previously by Quinn et al. [30] by obtaining the surface pressure isotherms of the Langmuir films. These authors assessed the amphipathic character of ubiquinone molecules and that their ability to penetrate the phospholipid monolayers increased as the isoprenoid chain length increases. This former study also reported that the characteristics of the mixed monolayers depend markedly on the surface pressure of the monolayer.

In the present work, mixed films of the phospholipid dipalmytoilphosphatidylcholine (DPPC) with the biologically significant quinone UQ have been studied at the molar ratios DPPC:UQ 5:1 and 10:1. These ratios, a bit higher but not too far from the biological ones, provides enough UQ concentration for a good analysis and for observing the influence of the lateral pressure on the UQ insertion in the DPPC matrix. In order to study the influence of the UQ in the DPPC film at different surface pressures, the Langmuir and LB techniques have been used [31, 32]. These techniques also allow us to control the film structure and the monolayer or multilayer formation, and surprisingly they have not been applied rigorously to these systems despite the fact that better quality layers can be assembled using the LB technique than by fusion of vesicles [15]. The use of several surface pressures allows us studying the influence of this parameter on the UQ location. Atomic Force Microscopy (AFM) has been used to characterize the organization at the nanometric/micrometric level of the LB films of DPPC, UQ and the DPPC:UQ mixtures. The redox behaviour of the LB films has been characterized

by cyclic voltammetry (CV) using ITO as working electrode, due to its optical and electrical properties and its hydrophilic character, being these properties more suitable for solar cells and artificial photosynthesis applications. Finally, we try to correlate the film formation and film structure with the redox response.

2. Experimental

2.1 Materials

Dipalmitoylphospatidylcholine (DPPC) was purchased from Avanti Polar Lipids and ubiquinone-10 (UQ) HPLC grade was from Sigma-Aldrich. KH_2PO_4, KCl and chloroform of analytical grade were used in solutions preparation. Water was ultrapure MilliQ® (18.2 MΩ·cm). Indium tin oxide deposited glass slides (ITO) were purchased to SOLEMS (France) and mica sheets to TED PELLA Inc (CA).

2.2 Monolayer formation

Langmuir and Langmuir-Blodgett (LB) monolayer formation were carried on a Nima model 1232D1D2 trough using MilliQ® quality water as subphase. Solutions of DPPC, UQ and DPPC:UQ were prepared using chloroform. LB monolayers were transferred to the corresponding substrate surface at defined surface pressures values (π). Barrier closing rates were fixed at 50 cm^2·min^{-1} (6.3 Å^2·molec^{-1}·min^{-1}) for isotherm registration and at 25 cm^2·min^{-1} (3.1 Å^2·molec^{-1}·min^{-1}) for LB film transfer. No noticeable influence of these compression rates was observed on the isotherm shape. Isotherm recording was carried out adding the solution to the subphase and waiting 15 minutes for perfect spreading. LB film transfer was conducted dipping the substrate (ITO slide or mica sheet) on the subphase before adding the solution and five minutes were lagged after pressure setpoint was achieved. Transfer speed was set at 5 mm/min linear velocity. Experiments were conducted at 22±1ºC.

2.3 AFM characterization

The AFM topographic images of LB films were acquired in tapping mode using a Multimode AFM controlled by a Nanoscope IV electronics (Veeco, Santa Barbara, CA). Silicon tips with a nominal spring constant of 40 nN·nm^{-1} were used (ACT-W, Applied Nanostructures, Santa

Clara, CA). Images were acquired at 1.5 Hz and at minimum vertical force so as to reduce sample damage.

2.4 Electrochemical characterization

The voltammetric measurements were performed in a conventional three-electrode cell using an Autolab Potentiostat-Galvanostat PGSTAT-12 (Ecochemie, NL). Working electrodes used were ITO slides (10mmx25mm) cleaned once with ethanol and three times with MilliQ® grade water. Counter electrode was a platinum wire in spiral geometry and the reference electrode was an Ag/AgCl/3M KCl microelectrode model DRIREF-2SH from WPI (World Precision Instruments). This reference electrode was mounted in a Lugging capillary containing KCl solution at the same cell concentration. All reported potentials were referred to this electrode. The electrochemical cell contained 0.150 M KCl as supporting electrolyte at pH=7.4 adjusted with the KH_2PO_4/K_2HPO_4 buffer. All solutions were freshly prepared with MilliQ® grade water and de-aerated with flow of Argon gas for 15 minutes prior the CV experiments, which were conducted at 22±1ºC. Voltammetric experiments were carried out at different scan rates, scanning towards negative potentials in a home-made glass cell with a reaction area of 33 mm^2.

3. Results

3.1 Surface pressure-area isotherms and AFM characterization

Figure 1 shows the surface pressure-area (π-A) isotherms for Langmuir films of DPPC, UQ and the DPPC:UQ 5:1 and 10:1 mixtures. The DPPC isotherm shows the known phase transition from liquid expanded (LE) to liquid condensed (LC) at low surface pressures (around 6 mN·m^{-1}), and a collapse at ca. 55 mN·m^{-1}. The UQ isotherm presents only a LE phase followed by a multilayer formation at a surface pressure of 11 mN·m^{-1}. In the isotherms of the DPPC:UQ mixtures the influence of UQ addition on the DPPC isotherm is strong compared with that of duroquinone [21] indicating a considerable incorporation of UQ in the DPPC matrix. In the isotherm we can distinguish three regions delimited by two inflexion points done at surface pressures of ca. 18 and 26 mN·m^{-1} for the 5:1 mixture and ca. 9 and 20 mN·m^{-1} for the 10:1 mixture. In order to investigate deeply the film structure in correspondence with the isotherm characteristics, LB films were transferred at selected surface pressure values onto mica and the corresponding AFM images where obtained. The

first region, from 0 to 18 mN·m^{-1} for the 5:1 mixture and from 0 to 9 mN·m^{-1} for the 10:1 mixture, corresponds to a DPPC:UQ mixed LE phase. Figure 2 shows AFM images of DPPC, UQ and the DPPC:UQ 5:1 and 10:1 mixtures, extracted at $\pi = 6$ mN·m^{-1}. The figure shows the strong influence of UQ molecules in the DPPC matrix. The UQ molecules difficult the LE to LC phase transition of the DPPC and consequently the formation of the more compact LC DPPC film. In the second region, for instance from 18 to 26 mN·m^{-1} for the 5:1 mixture, a condensation of the monolayer takes place (see Figure 3), with interaction either between DPPC molecules as between UQ and DPPC molecules. As the interaction between identical DPPC molecules is stronger than the interaction between dissimilar UQ and DPPC molecules, the UQ molecules may be progressively expelled from the DPPC matrix. This expulsion occurs mainly at the second inflexion point. The last region, above 26 mN·m^{-1} for the 5:1 mixture and above 20 mN·m^{-1} for the 10:1 mixture, resembles the pure DPPC isotherm, indicating that has been partially expelled and the DPPC matrix is leading the isotherm shape. At a surface pressure value of 40 mN·m^{-1}, part of the expelled UQ molecules form clusters above the DPPC monolayer before DPPC collapse, as can be seen clearly for the 5:1 mixture in the corresponding AFM image of Figure 3.
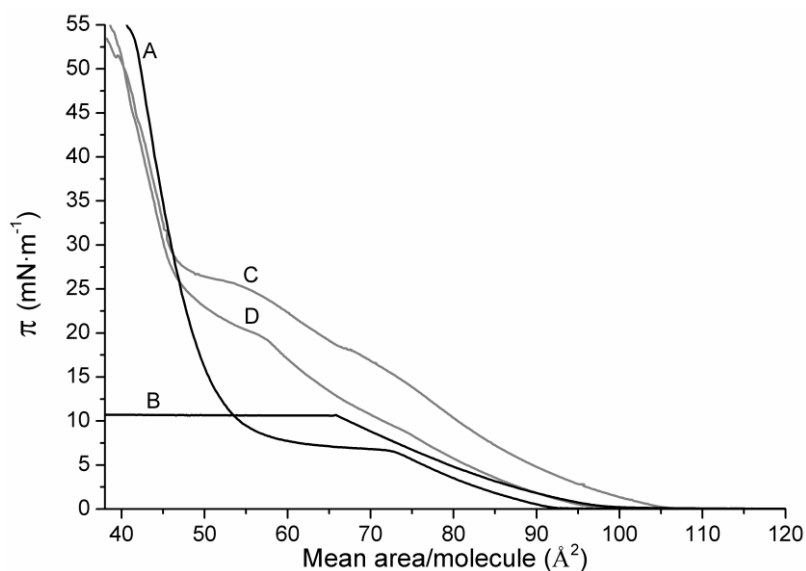
Figure 1. π-A isotherms for DPPC, UQ and DPPC:UQ 5:1 and 10:1 mixtures at 22ºC. Black lines are pure components a) DPPC b) UQ. Grey lines are the DPPC:UQ mixtures c) 5:1 d) 10:1.
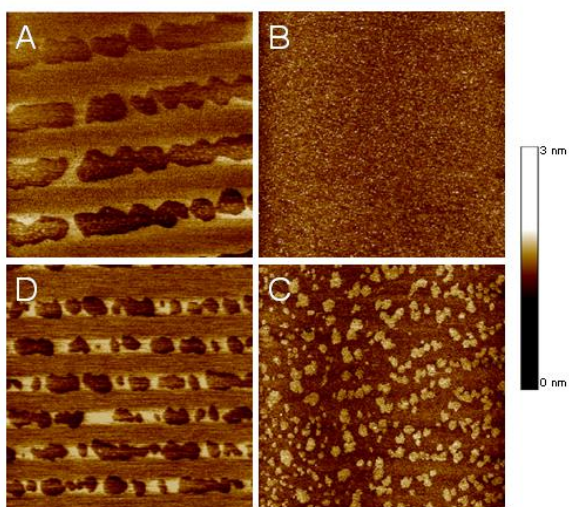
Figure 2. AFM images (5 μm x 5 μm) of LB films transferred on mica at π = 6 mN·m^{-1} for A) DPPC, B) UQ and DPPC:UQ mixtures C) 5:1 and D) 10:1 at 22ºC.
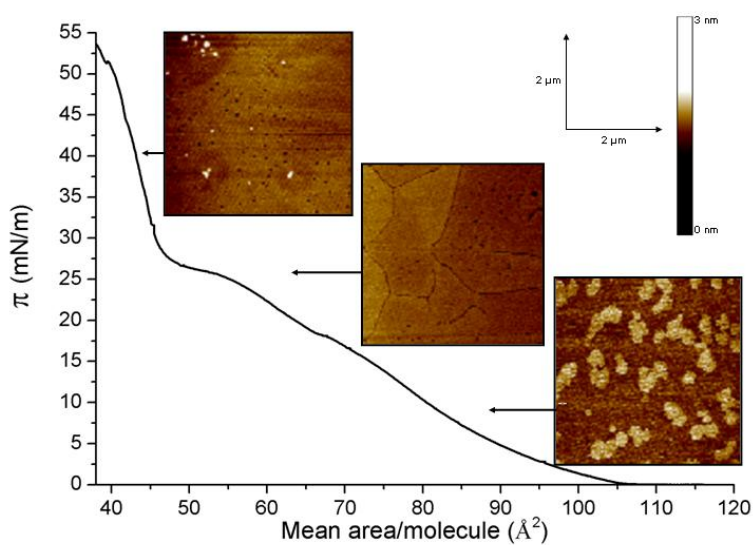

Figure 3. AFM images (2μm x 2 μm) of LB films transferred on mica for DPPC:UQ 5:1 mixture at π = 6, 25 and 40 mN·m^{-1} at 22ºC.

3.2 Cyclic Voltammetric study of the LB films on ITO

ITO/electrolyte and ITO-DPPC/electrolyte systems

LB films of DPPC transferred on ITO at selected surface pressures were studied using cyclic voltammetry in a 0.150 M KCl cell solution buffered at pH=7.4, in order to estimate the electrode/electrolyte interface capacitance (C_d) from the values of the voltammetric charging current [33]. A bare ITO electrode used as a blank system, shows no redox response in the experimental potential working range from 1.000 V to -0.700 V (see blank curve in Figure 4), having a C_d around 1 µF·cm^{-2}. The ITO-DPPC electrode presents values of C_d slightly higher, being between 2 to 2.8 µF·cm^{-2} for a potential range of 1.000 V to -0.400 V (see blank curves in Figures 5 and 6). This result indicates that the ITO-DPPC surface is more permeable, accessible, to the electrolyte ions than the bare ITO electrode surface. These values of C_d also indicate that the lipid layer presents few defects. Typical values of 1.7-1.8 µF·cm^{-2} have been reported for well made lipid monolayers [9] and around 6 µF·cm^{-2} for defective lipid bilayers [15]. At more cathodic potentials than -400 mV a continuous increase of the capacitance charging current values is obtained for the ITO-DPPC electrodes indicating that hydrogen evolution becomes important, in accordance with Yang et al.[10].

ITO-UQ/electrolyte system

LB films of pure UQ have been transferred on ITO electrode at two surface pressures, being chosen π = 6 (not fully compact UQ Langmuir film) and π = 11 mN·m^{-1} (fully compact UQ Langmuir film, just previous the multilayer formation region). Figure 4 shows the cyclic voltammetric behaviour of both LB films in the cell solution, having a main reduction (I_R) and oxidation (I_O) peaks in the interval between 0.400 and -0.400 V (cyclic voltammogram shown in the inset of Figure 4). If the potential is scanned to more negative potentials a second reduction peak (II_R) appears for the pure UQ LB film deposited at high pressure with its corresponding oxidation peak (II_O) in the reversing scan. Electrochemical processes I and II show irreversible behaviour with peak potentials $E_{pR}(I)$= -0.300 $\pm$ 0.010 V, $E_{pR}(II)$= –0.580 $\pm$ 0.010 V, $E_{pO}(I)$= 0.260 $\pm$ 0.010 V, $E_{pO}(II)$= 0.760 $\pm$ 0.020 V. The formal reduction potential referred to the Ag/AgCl/ KCl (3M) reference electrode can be calculated by taking the average of the reduction and oxidation peak potentials being $E_f(I)$=-0.020 $\pm$ 0.020 V for the process I and $E_f(II)$= 0.090 $\pm$ 0.020 V for the process II.
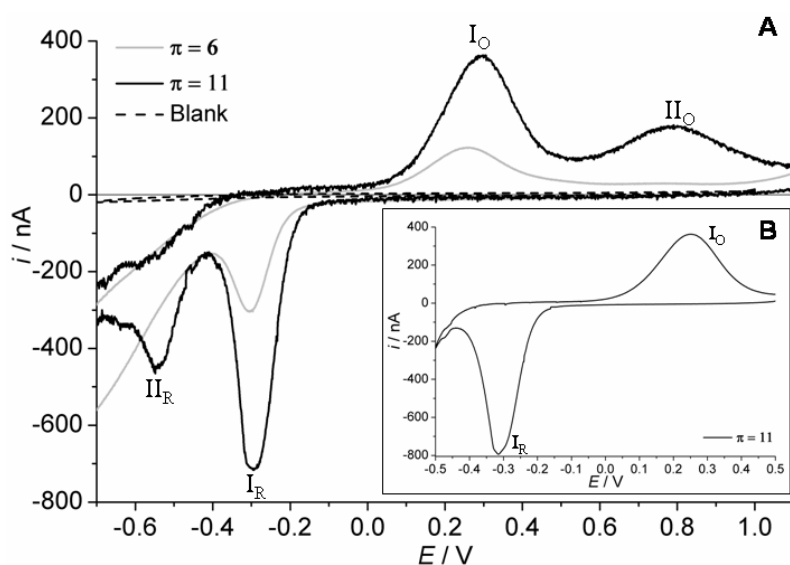
Figure 4. A) Cyclic voltammogram of UQ LB film at $\pi = 6$ and 11 mN·m^{-1}. Dashed line represents CV of bare ITO electrode. B) CV of UQ LB film transferred at π=11 mN·m^{-1} in short potential working screen. Both experiments were carried in a 0.150 M KCl electrochemical cell using potassium phosphate buffered solution at pH 7.4 at a scan rate of 10 mV·s^{-1}.

ITO-DPPC:UQ/ electrolyte systems

LB films of the DPPC:UQ 5:1 and 10:1 mixtures have been also transferred at selected surface pressures on ITO to characterize the redox behaviour of the DPPC:UQ mixtures at different compression states of the film. A good reproducibility of the voltammetric response is obtained in all cases from the third scan and at least 15 cycles.

Figures 5A and 5B show the cyclic voltammetry for both DPPC:UQ 5:1 and 10:1 mixtures, respectively, at the low surface pressures of 6 and 15 mN·m^{-1}. In this region, only a main irreversible process is obtained with wide reduction and oxidation peaks and peak potentials $E_{pR}(I)$= -0.250 ± 0.020 V and $E_{pO}(I)$= 0.170 ± 0.020 V. The electrochemical process gives a formal potential $E_f(I)$= -0.040 ± 0.020 V close to that of process I seen for pure UQ monolayers, so we labelled it also as process I.

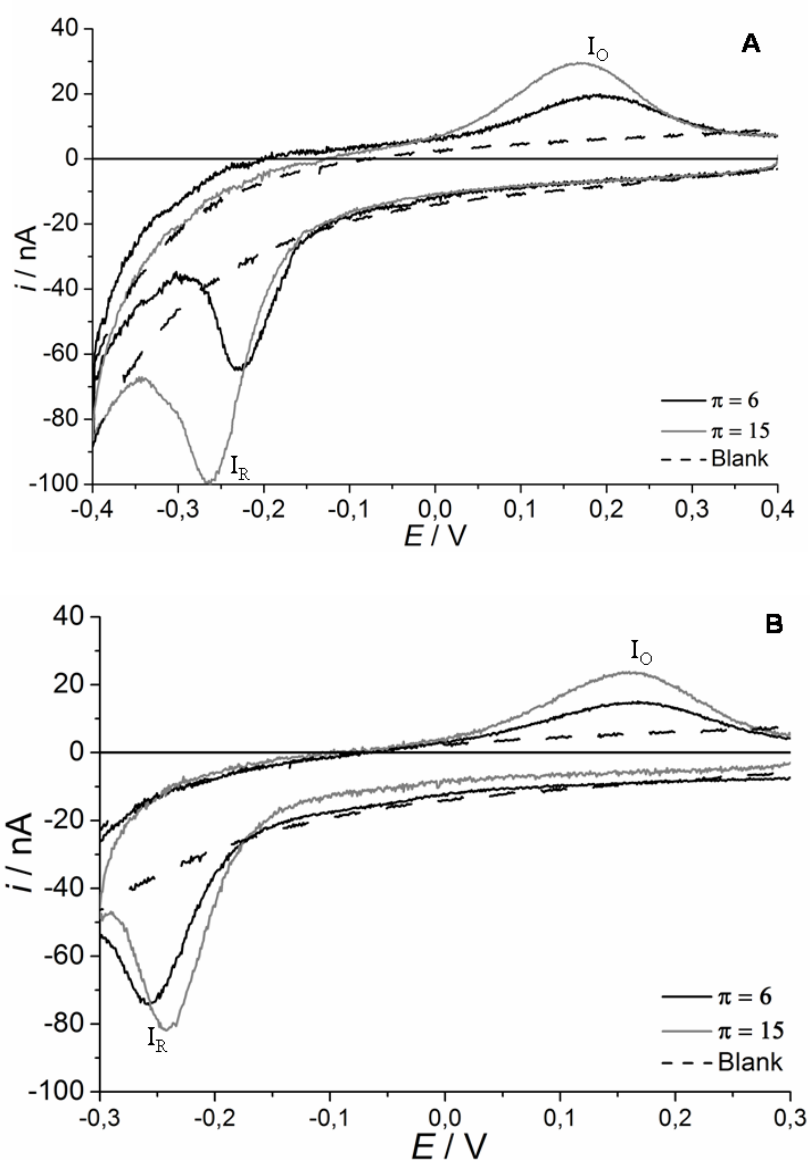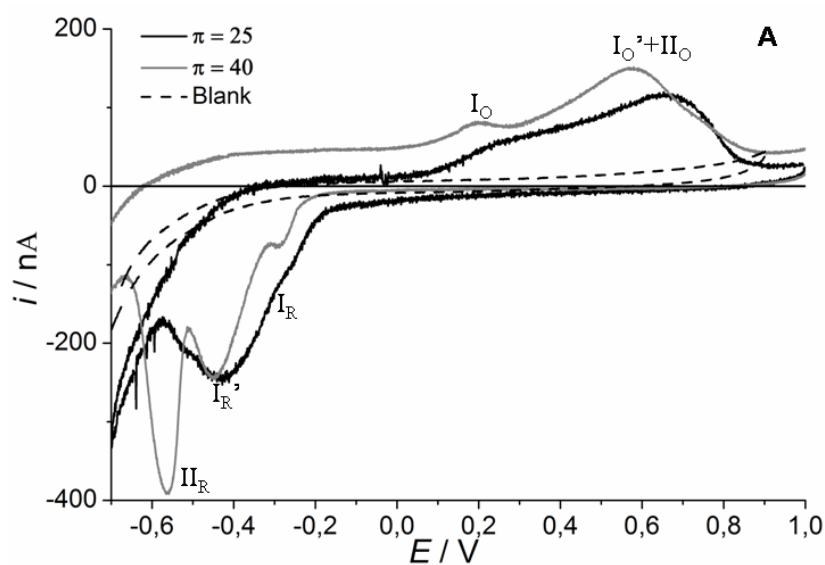Figure 5. Cyclic voltammograms of DPPC:UQ LB films at π = 6 and 15 mN·m⁻¹. Dashed line represents the CV of the ITO/DPPC electrode at π = 6 mN·m⁻¹. A) DPPC:UQ 5:1 mixture. B) DPPC:UQ 10:1 mixture. All these experiments were carried in a 0.150 M KCl electrochemical cell using potassium phosphate buffered solution, pH 7.4, at a scan rate of 10 mV·s⁻¹.

Figures 6A and 6B represents the cyclic voltammograms for both DPPC:UQ 5:1 and 10:1 mixtures, respectively, at medium, 25 mN·m⁻¹, and high, 40 mN·m⁻¹, surface pressures. For the DPPC:UQ 5:1 mixture, at π = 25 mN·m⁻¹ a wide reduction peak, that draws three waves, and two wide oxidation peaks are obtained and at π = 40 mN·m⁻¹ three reduction peaks are clearly differentiated in the cathodic scan and two oxidation peaks in the anodic scan. In Figure 6A, the peaks have been labelled as processes I_R, I_R' and II_R, for the cathodic scan and

10

I_O and $I_O´+II_O$ for the anodic scan. The assignment of reduction peaks I_R and II_R and oxidation peak I_O has been made taking as a reference the peak potentials of Figure 4 for the ITO/UQ system. For the DPPC:UQ 10:1 mixture, either at $\pi = 25$ mN·m^{-1} or at $\pi = 40$ mN·m^{-1} two reduction and oxidation peaks are obtained (Figure 6B), labelled as processes I_R, $I_R´$, for the cathodic scan and I_O, $I_O´$ for the anodic scan in comparison with Figure 6A. For process I, the reduction and oxidation peak potentials and the formal potential of $E_f(I)$ matches with those obtained for the LB films of pure UQ and DPPC:UQ at low surface pressure values (Figures 4 and 5). The new peak $I_R´$ appears at $E_{pR}(I') = -0.430 \pm 0.020$ V in the cathodic scan. In the anodic scan, a clear oxidation peak at $E_{pO}(I') = 0.420 \pm 0.010$ V is obtained for DPPC:UQ 10:1 mixture (Figure 6B) and a formal potential of $E_f(I') = -0.005 \pm 0.010$ V can be calculated for process I'. Figure 6A shows a clear reduction peak potential at $E_{pR}(II) = -0.580 \pm 0.010$ V for process II at $\pi = 40$ mN·m^{-1} obtained in the cathodic scan, that matches with the value obtained from Figure 4. The peak labelled $I_O´+II_O$ is wide, asymmetric and appears at less anodic potentials than the peak II_O in Figure 4, which indicates that is the contribution of both processes I' and II.
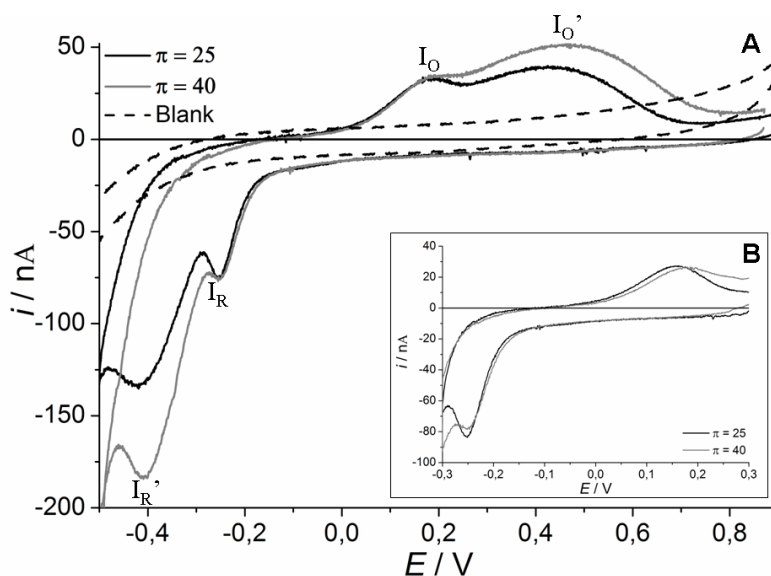
Figure 6. Cyclic voltammogram of DPPC:UQ LB films at π = 25 and 40 mN·m⁻¹. Dashed line represents CV of ITO-DPPC electrode at π = 40 mN·m⁻¹. A) DPPC:UQ 5:1 mixture. B) DPPC10:1 mixture. C) DPPC:UQ 10:1 mixture in short potential working screen. All these experiments were carried in a 0.150 M KCl electrochemical cell using potassium phosphate buffered solution, pH 7.4, at a scan rate of 10 mV·s⁻¹.

4. Discussion

The shape of the voltammograms shown in Figures 4-6 presents important deviations respect to an ideal reversible system, according to the theoretical models proposed in the literature to describe the cyclic voltammetric response of a surface confined reaction [34-36]. Main features are that the peak shape is not symmetrical, being the reduction peaks sharper than the oxidation ones, and that the separation between reduction an oxidation peak potentials is large. Such deviations are attributed [36, 37] to the interactions between the electroactive centres, to the not homogeneous spatial distribution of the centres and to the non-equivalent sites in the film.

Further information of the ITO/UQ or ITO/DPPC:UQ electrochemical systems have been performed using cyclic voltammetry at different scan rates. Figure 7A, 7B and 7C show the peak current variation with the potential scan rate for the electrochemical processes presented in Figures 4-6. A good linear dependence is obtained either for processes I, I' or II, indicating that UQ molecules are surface confined species [34] and the processes are not diffusion controlled. On the other hand, a linear variation of the peak potential with the logarithm of the

12

scan rate, not shown, is obtained in all cases which confirm that irreversible reactions of these surface confined molecules take place [38].
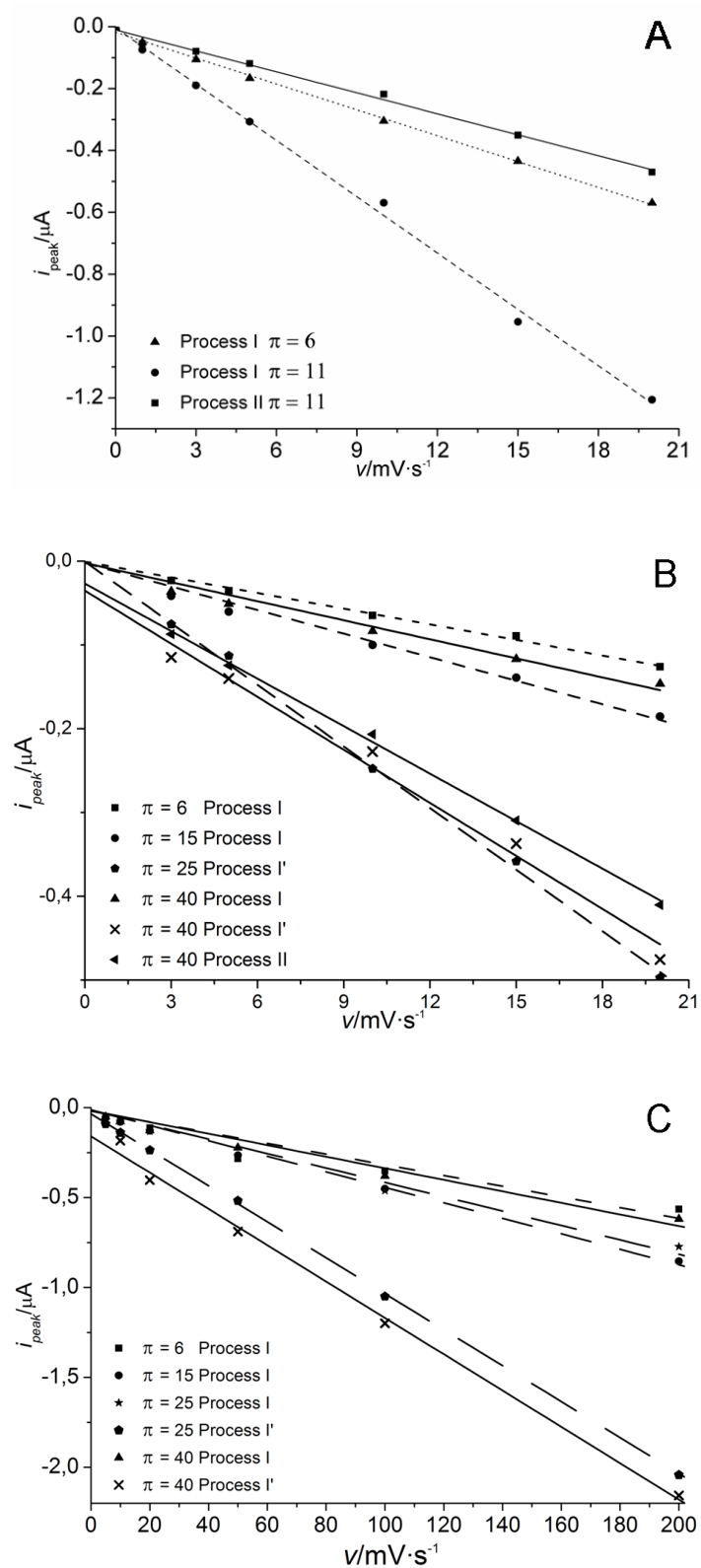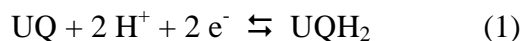

Figure 7. Peak intensity vs. the scan rate for: A) ITO/ UQ at $\pi = 6$ and 11 mN·m^{-1}, B) ITO/ DPPC:UQ 5:1 at $\pi = 6$, 15, 25 and 40 mN·m^{-1} and C) ITO/ DPPC:UQ 10:1 at $\pi = 6$, 15, 25 and 40 mN·m^{-1}

The overall reaction of charge transfer of the couple UQ/UQH$_2$, is:

$$UQ + 2\,H^+ + 2\,e^- \leftrightarrows UQH_2 \qquad (1)$$

The values of E_f obtained for the ITO/UQ or ITO/DPPC:UQ electrochemical systems are more positive than those reported for the UQ/UQH$_2$ system adsorbed on mercury electrodes [8, 39] (-0.11 vs Ag/AgCl, KCl (3M), pH=7) or supported in a lipid monolayers on mercury [5, 8, 27] (-0.29, -0.09, -0.14, respectively, vs Ag/AgCl, KCl (3M), pH=7). On the other hand, our values are more similar to that of the Benzoquinone/hydroquinone system in aqueous solution (0.08 vs Ag/AgCl, KCl (3M), pH=7) than in an aprotic solvent (-0.51 and -1.37 vs Ag/AgCl, KCl (3M)) [34]. These values could indicate that in our system, the UQ molecules have H$^+$ ions more available.

Focussing the attention in the orientation of UQ molecules in the LB monolayers transferred to ITO, it is expected that UQ molecules inserted in the phospholipid monolayer orient the quinone head to the hydrophilic ITO surface and this situation is also expected for the pure UQ monolayer with their head groups directed toward the surface. Therefore, for the ITO/UQ system, we correlate process I in Figure 4 with the redox electron transfer of the UQ/UQH$_2$ quinone centres of the monolayer directly attached to the ITO electrode surface. According to the isotherm of pure UQ molecules shown in Figure 1, this is the main situation for UQ monolayers transferred on ITO at surface pressure lower than 11 mN·m^{-1}. When the UQ LB monolayer is extracted around the collapse pressure, process II appears in the voltammogram of Figure 4, at more cathodic potentials than process I. Process II is more irreversible than process I, but have a more positive formal potential (close to that of benzoquinone/hydroquinone in aqueous solution) that can be correlated with a more aqueous environment for the UQ head group. As the monolayer transference around the collapse pressure is slightly unstable and may produce some UQ expelling during the LB transfer, effect which is difficult to appreciate in AFM images, we correlate peak II with the electron transfer of the UQ molecules that have been expelled and are laying over the monolayer.

Analysing the ITO/DPPC:UQ system, the experimental surface coverage of the UQ molecules for the total reduction, Γ_R, and oxidation, Γ_O, processes shown in Figures 4-6, can be

calculated integrating the area under the reduction and oxidation waves, and considering the overall reaction of charge transfer of the couple UQ/UQH_2 described in (1) . We have taken the Γ_O value as the experimental surface coverage value, because the ratio Γ_R/Γ_O is slightly greater than the unity due to the hydrogen evolution process that takes place in the cathodic scan. The Γ_O values are reported in Table I. On the other hand, we have also determined the contribution of the oxidation charge corresponding only to process I on Figures 5-6 and calculated the Γ_O (I) values for the different DPPC:UQ films. Γ_O (I) values are represented in Figure 8 vs. the surface pressure. At low surface pressures, when only process I is present in the voltammograms, the Γ_O (I) values are equal to the total Γ_O values (Table I), but increasing surface pressure, when peaks I' and II appear, Γ_O (I) attains a maximum value, whereas Γ_O continues increasing.

Table I. Experimental and expected total surface coverage involved in the redox process for ITO/UQ and ITO/DPPC:UQ systems. Experiments were carried at a scan rate of 10 mV·s^{-1} in a 0.150 M KCl solution buffered at pH 7.4 using KH_2PO_4/K_2HPO_4.

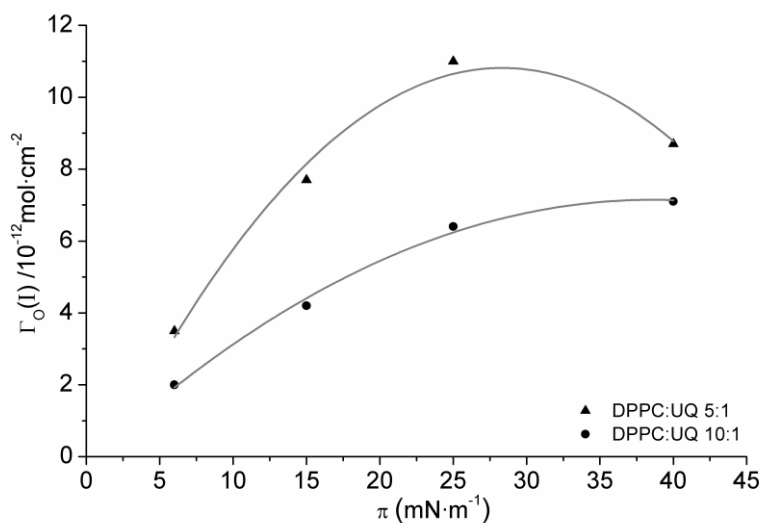| ITO/UQ system			
π (mN·m^{-1})	$\Gamma_O/10^{-12}$mol·cm^{-2}	Γ_{expect} / 10^{-12}mol·cm^{-2}	Electroactive Fraction
6	37.5	145.5	25.8 %
11	149.2	255.4	58.4 %
ITO/DPPC:UQ 5: 1mixture system			
6	3.5	21.3	16.5 %
15	7.7	37.9	20.3 %
25	33.9	49.4	68.6 %
40	55.8	62.9	88.7 %
ITO/DPPC:UQ 10: 1mixture system			
6	2.0	12.9	15.8 %
15	4.2	24.1	17.3 %
25	17.1	31.8	53.8 %
40	24.0	35.5	67.6 %

Figure 8. Surface coverage of the UQH$_2$ fraction oxidized via process I, Γ_O (I), vs surface pressure, π, for DPPC:UQ 5:1 and DPPC:UQ 10:1 mixtures.

Correlating the above information with the surface pressure isotherms represented in Figure 1, when DPPC:UQ LB films are extracted at low surface pressures (lower than 18 mN·m^{-1} for DPPC:UQ 5:1 mixture and lower than 9 for DPPC:UQ 10:1 mixture) a mixed monolayer in a LE phase is formed on the ITO surface, with the structure shown in the AFM image in Figure 3 at $\pi=$ 6 mN·m^{-1}. In these cases, processes labelled as I are mainly observed in the voltammograms (Figure 5). As the formal potential of process I correlates with that obtained for ITO/UQ system, we describe this process as the redox electron transfer of the UQ/UQH$_2$ quinone centres directly attached to the ITO electrode surface that are distributed inside the DPPC matrix.

When the DPPC:UQ LB films are extracted at a medium surface pressure, within the range 18 to 26 mN·m^{-1} for DPPC:UQ 5:1 mixture and 9 to 20 mN·m^{-1} for DPPC:UQ 10:1 mixture, the tendency of DPPC molecules to pack itself, changing from a LE to a LC phase, can promote that UQ molecules adopt different orientations respect to those at lower surface pressures. When two reduction peaks (Figure 6 at $\pi=$ 25 mN·m^{-1}) are mainly obtained in the voltamograms, we postulate that the UQ molecules are distributed inside the DPPC matrix mainly in two kind of orientations. A fraction, Γ_O(I), is reduced via process I. This fraction corresponds to molecules directly attached to the electrode surface. The rest of molecules are reduced via the process I' that has a peak potential in between the peak potentials of processes I and II. Process I' is more irreversible than process I and E_f(I') is more positive than E_f(I).

16

This suggest that the quinone head of these UQ molecules are not attached to the electrode surface, they are placed in an environment with H$^+$ ion more available nearer to the aqueous electrolyte but still inside the DPPC matrix, according to the surface pressure isotherms shown in Figure 1 and the structural organization of the monolayer shown in the AFM image in Figure 3 at π= 25 mN·m^{-1}. The second inflexion point shown in the isotherms for DPPC:UQ mixtures indicates the surface pressure in which the expulsion of the UQ molecules from the DPPC matrix begins to take place. When the DPPC:UQ LB film is extracted at surface pressures above the second inflexion point two or three peaks I, I' and II can be obtained (Figure 6 at π= 40 mN·m^{-1}). Peaks I and I' are correlated, respectively, with the described DPPC:UQ organization explained above. As the reduction potential of peak II correlates with those obtained for ITO/UQ system, we describe this process as the redox electron transfer of the UQ/UQH$_2$ quinone centres located over the first DPPC:UQ monolayer forming clusters or islands (bright circles in AFM image in figure 3 at π= 40 mN·m^{-1}). The organization of the UQ in the DPPC matrix is depicted schematically in Scheme 2.
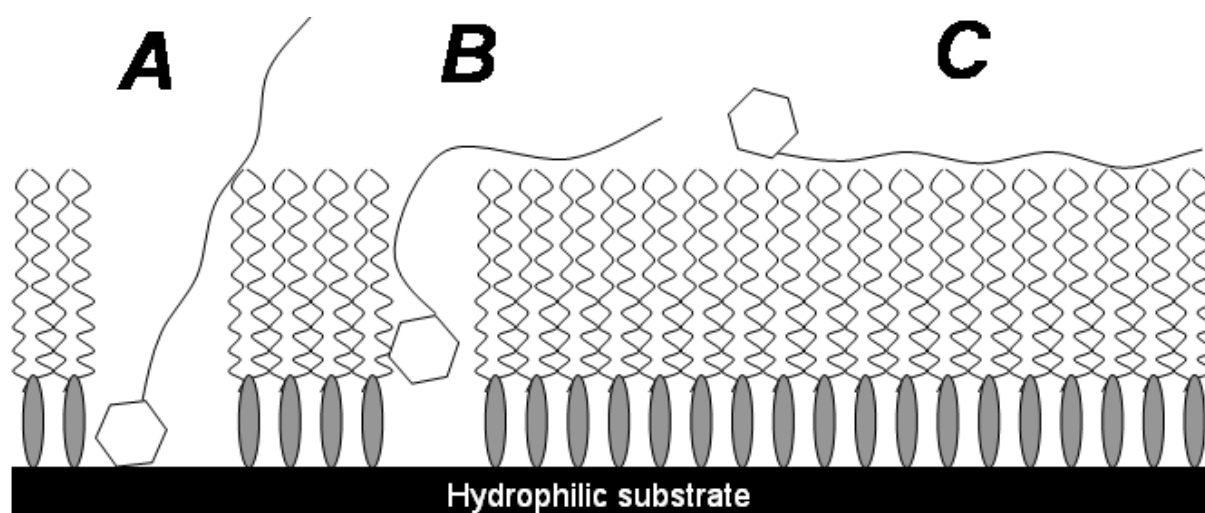
Scheme 2

Scheme 2. UQ organization in the DPPC matrix on ITO. Organization A is related to the UQ fraction that experiments redox process I; organization B is related to UQ fraction that experiments redox process I' and organization C is related to UQ molecules, outside the DPPC matrix, that experiment redox process II.

In a recent study of the UQ/UQH$_2$ in phospholipid monolayers on mercury [6], Becucci et al. have proposed a reaction pathway describing the overall reaction (1) and have obtained an

increase in the separation between oxidation and reduction peaks when increasing the UQ surface concentration, that have explained by an increase in the attractive lateral interactions between molecules of the same specie. This effect caused the peaks become more acute. A similar behaviour is obtained in our study for the DPPC:UQ LB monolayers on ITO but in our case the increase of the UQ surface concentration is obtained increasing the surface pressure in which the monolayer is formed. This let us to think that a similar reaction pathway could apply in our system.

Additional information of the electrochemical behaviour of our system can be obtained calculating a maximum UQ surface coverage expected for each system, Γ_{expect}, from the corresponding value of the mean area per molecule extracted from Figure 1 (Table I). Γ_{expect}, has been calculated assuming a perfect LB transfer (except at surface pressure $\pi=6$, which is around 70%), that the DPPC an UQ molecules are perfectly mixed in the Langmuir monolayer and that the UQ molecules represent a molar fraction of 16.7% (5:1) and 9.1% (10:1) in this perfect mixed monolayer. Table I shows that the experimental total surface coverage is lower than the expected, for each system. Therefore, not all the expected UQ confined redox centres have been reduced during the period of potential scan, and an electroactive fraction is calculated. Similar behaviour has also been observed by Laval et al. [19], studying UQ reduction and in other LB redox systems [36, 37] and is explained due to different factors: a non homogeneous electrode surface, a non homogeneous distribution of the redox centres in the film where not all the sites are equivalent or where some redox centres are not in direct contact with the electrode surface. In our case we attribute this behaviour to the use of an ITO electrode which presents semiconductive properties and then behaves different than metal electrodes as gold or mercury.

4. Conclusion

Surface pressure-area isotherms of DPPC and DPPC:UQ 5:1 and 10:1 Langmuir films show a great influence of UQ in the isotherm shape, in respect to that of DPPC. AFM images of LB films transferred at several surface pressures reveal interesting features at the nanometric scale of the UQ organization in the DPPC matrix. At low surface pressures UQ becomes placed in between DPPC matrix, but at high surface pressures UQ molecules are progressively squeezed out from the monolayer. Cyclic voltammetry has been used to study the redox response of the UQ molecules influenced by the phospholipid environment. The

cyclic voltammograms of the DPPC:UQ LB films present a number of peaks and a shape that depends on the transfer surface pressure, revealing that the electron transfer is strongly influenced by the film structure. The electrochemical response has been correlated with the surface pressure-area isotherms and AFM images, corroborating that the UQ molecules are located in different kind of equivalent sites in the DPPC monolayer. The proportion of such equivalent sites depends on the transfer surface pressure of the LB films.

Acknowledgements

References

[1] E. Swiezewska, G. Dallner, B. Andersson and L. Ernster, J. Biol. Chem. 268 (1993) 1494-1499.

[2] M. Jemiola-Rzeminska, J. Kruk, M. Skowronek and K. Strzalka, Chem. Phys. of Lipids, 79 (1996) 55-63.

[3] H. Ti Tien and Angelica L. Ottova, Journal of Membrane Science, 189 (2001) 83–117.

[4] A. Nelson, Current Opinions in Colloid and Interface Science, 15 (2010) 455-466.

[5] M.R. Moncelli, L. Becucci, A. Nelson, R. Guidelli. Biophys. J. 70 (1996) 2716-2726.

[6] L. Becucci, F. Scaletti, R. Guidelli. Biophys. J. 101 (2011) 134-143

[7] G. J. Gordillo and D. J. Schiffrin, J. Chem. Soc. Faraday Trans. 90 (1994) 1913-1922.

[8] G. J. Gordillo and D. J. Schiffrin, Faraday Discuss. 116 (2000) 89-107

[9] R. Guidelli, G. Aloisi, L. Becucci, A. Dolfi, M. R. Moncelli, F. T. Buoninsegni, J. Electroanal. Chem., 504 (2001) 1-28.

[10] J. Yang and M. Kleijn, Biophysical J. 76 (1999) 323-332.

[11] J. Kruk, K. Strzalka and R-M. Leblanc, Biochem. Biophys. Acta, 1142 (1993) 6-10.

[12] Z. V. Leonenko, E. Finot, H. Ma, T.E. S. Dahms and T. Cramb, Biophys. J. 86 (2004) 3783-3793.

[13] I. Zawisza, X. Bin, J. Lipkowski, Bioelctrochem, 63 (2004) 137-147

[14] I. Zawisza, X. Bin, J. Lipkowski, Langmuir, 23 (2007) 5180-5194

[15] J. Lipkowski, Phys. Chem. Chem. Phys., 42 (2010) 13874-13887.

[16] J. T. Woodward, C. W. Meuse, J. Colloid Interface Sci. 334 (2009) 139-145.

[17] T. A. Oleson, N. Sahai, J. Colloid Interface Sci. 352 (2010) 316-326.

[18] M. Anderson, J. Jackman, D. Wilson, P. Jarvoll, V. Alfredson, G. Okeyo, R. Duran, Colloids and Surf. B: Biointerfaces, 82 (2011) 550-561.

[19] J-M Laval and M. Madja, Thin Solid Films, 244 (1994) 836-840.

[20] E. Torchout, C. Bourdillon, J-M Laval, Biosensors and Bioelectronics, 9 (1994) 719-723.

[21] 10 J. Hoyo-Pérez, J. Torrent-Burgués and F. Sanz-Carrasco, Proceedings of the SIBAE 2010, Alcala de Henares, Spain.

[22] Y. Suemori, M. Nagata, M. Kondo, S. Ishigure, T. Dewa, T. Ohtsuka and M. Nango, Colloid Surf. B: Biointerfaces, 61 (2008) 106-112.

[23] S. Sanchez, A. Arratia, R. Córdova, H. Gómez, R. Schrebber, Bioelectrochemistry and Bioenergetics, 36 (1995) 67-71.

[24] H. Park, J-S. Park and Y-B. Shim, J. Electroanal. Chem. 438 (1997) 113-119.

[25] H. Shiba, K. Maeda, N. Ichieda, M. Kasuno, Y. Yoshida, O. Shirai, S. Kihara. J. Electroanal. Chem. 556 (2003) 1-11.

[26] E. Torchout, J-M Laval, C. Bourdillon, M. Madja, Biophys. J., 66 (1994) 753-762.

[27] D. Marchal, W. Boireau, J. M. Laval, J. Moiroux, C. Bourdillon, Biophys. J. 72 (1997) 2679-2687.

[28] D. Marchal, W. Boireau, J. M. Laval, J. Moiroux, C. Bourdillon, Biophys. J. 74 (1998) 1937-1948.

[29] V. Mirceski; R. Gulaboski, I. Bogeski and M. Hoth, J. Phys. Chem. 111 (2007) 6068-6076.

[30] P. J. Quinn and M. A. Esfahani, Biochem. J. 185 (1980) 715-722.

[31] O.Domenech, J.Torrent-Burgués, S. Merino, F. Sanz, M.T. Montero, J. Hernández-Borrell. Colloid Surf. B: Biointerfaces, 41(2005) 233-238.

[32] J. Torrent-Burgués, G. Oncins and F. Sanz, Contribute. Sci. 4 (2008) 177-186.

[33] E. Guaus, A. Errachid, J. Torrent-Burgués. J. Electroanal. Chem. 614 (2008) 73-82.

[34] A. J. Bard and L. R. Faulkner, Electrochemical methods. Fundamentals and applications, John Wiley& Sons, NY, 2001.

[35] E. Laviron, J. Electroanal. Chem. 101 (1979) 19-28.

[36] H. Daifuku, K. Aoki, K. Tokuda and M. Matsuda, J. Electroanal. Chem. 183 (1985) 1-26.

[37] L. M. Goldenberg, J. Electroanal. Chem. 379 (1994) 3-19.

[38] E. Laviron in: J. Bard, I, Rubinstein (EDS.), Electroanalytical Chemistry, vol. 12, Marcel Dekker, New York, 1982.

[39] S. Sek asnd R. Bilewicz, J. Inclusion Phenom. Macrocyclic Chem, 35 (1999) 55-62.